Article

Catalytic Oligomerization of Ethylene to Higher Linear α-Olefins Promoted by the Cationic Group 4 [(η5-Cp-(CMe-bridge)-Ph)M(ethylene)] (M = Ti, Zr, Hf) Active Catalysts: A Density Functional Investigation of the Influence of the Metal on the Catalytic Activity and Selectivity

Sven Tobisch, and Tom Ziegler

J. Am. Chem. Soc., **2004**, 126 (29), 9059-9071• DOI: 10.1021/ja048861l • Publication Date (Web): 03 July 2004

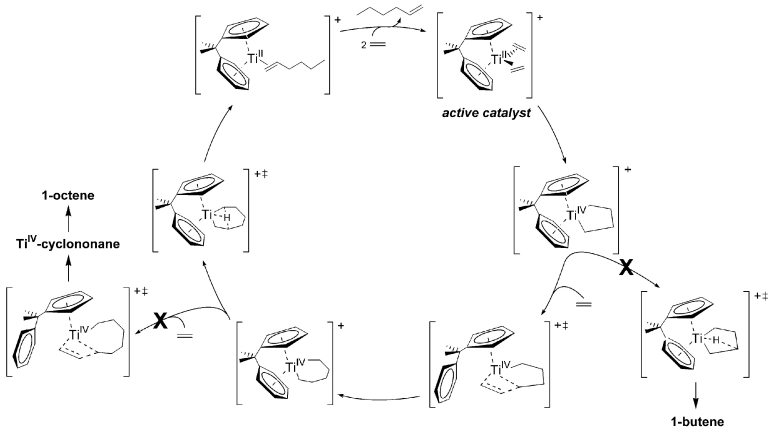

More About This Article

Additional resources and features associated with this article are available within the HTML version:

- Supporting Information
- Links to the 5 articles that cite this article, as of the time of this article download
- Access to high resolution figures
- Links to articles and content related to this article
- Copyright permission to reproduce figures and/or text from this article

View the Full Text HTML

J|A|C|S
ARTICLES
Published on Web 07/03/2004

Catalytic Oligomerization of Ethylene to Higher Linear α-Olefins Promoted by the Cationic Group 4 $[(\eta^5\text{-Cp-}(CMe_2\text{-bridge})\text{-Ph})M^{II}(\text{ethylene})_2]^+$ (M = Ti, Zr, Hf) Active Catalysts: A Density Functional Investigation of the Influence of the Metal on the Catalytic Activity and Selectivity

Sven Tobisch*,† and Tom Ziegler‡

Contribution from the Institut für Anorganische Chemie der Martin-Luther-Universität Halle-Wittenberg, Fachbereich Chemie, Kurt-Mothes-Strasse 2, D-06120 Halle, Germany, and Department of Chemistry, University of Calgary, University Drive 2500, Calgary, Alberta, Canada T2N 1N4

Received February 29, 2004; E-mail: tobisch@chemie.uni-halle.de

Abstract: A detailed theoretical analysis is presented of the catalytic abilities of heavier group 4 (M = Zr, Hf) metals for linear ethylene oligomerization with the cationic $[(\eta^5\text{-}C_5H_4\text{-}(CMe_2\text{-bridge})\text{-}C_6H_5)M^{IV}(CH_3)_2]^+$ complex as precatalyst, employing a gradient-corrected DFT method. The parent Ti system has been reported as a highly selective catalyst for ethylene trimerization. The mechanism involving metallacycle intermediates, originally proposed by Briggs and Jolly, has been supported by the present study to be operative for the investigated class of group 4 catalysts. Metallacycle growth through bimolecular ethylene uptake and subsequent insertion is likely to occur at uniform rates for larger cycles that are furthermore comparable for Ti, Zr, and Hf catalysts. Ethylene insertion into the two smallest five- and seven-membered cycles is found to become accelerated for Zr and Hf catalysts, which is due to geometrical factors. In contrast, electronic effects act to raise the barrier for metallacycle decomposition, affording α-olefins upon descending group 4. This process is furthermore predicted to be kinetically more difficult for larger metallacycles. The oligomer distribution of the Zr-mediated reaction is likely to comprise predominantly 1-hexene together with 1-octene, while 1-butene and α-olefins of chain lengths $C_{10}-C_{18}$ should occur only in negligible portions. A similar composition of α-olefins having C_6-C_{18} chain lengths is indicated for the Hf catalysts, but with long-chain oligomers and polymers as the prevalent fraction. Between the group 4 catalysts of the investigated type, the Zr system appears as the most promising candidate having catalytic potential for production of 1-octene, although not selectively. The influence of temperature to modulate the oligomer product composition has been evaluated.

Introduction

Higher linear α-olefins of chain lengths C_4-C_{18} are of utmost importance for the chemical industry as they are highly valuable and versatile feedstocks and building blocks for a variety of refining processes.[1] They are of wide interest as monomers (C_{10} for production of poly-α-olefins), as comonomers (C_4-C_8 to generate linear low-density LLDPE[2] polyethylene and as additives for high-density HDPE polyethylene production) in catalytic olefin polymerization,[1,3] and for production of surfactants ($C_{10}-C_{18}$).[1c,e] The use of higher linear α-olefins has been furthermore advanced to hydroformylation (C_6-C_{10}), affording straight-chain alcohols as well as to the manufacturing of plasticizers (C_6-C_{10}).[1c,e] Nowadays, oligomerization of the less expensive ethylene is the predominant route to α-olefins.[1c,e,4]

A variety of catalysts are known that actively promote the oligomerization of ethylene.[5,6] The majority of them afford a mixture of linear α-olefins having different chain lengths that usually obey a Schulz−Flory distribution.[7] The selective oligomerization to yield a specific higher linear α-olefin is highly

† Martin-Luther-Universität Halle-Wittenberg.
‡ University of Calgary.

(1) (a) Weissermal, K.; Arpe, H.-J. In *Industrial Organic Chemistry. Important Raw Materials and Intermediates*; Verlag Chemie: Weinheim, Germany, 1978. (b) Parshall, G. W.; Ittel, S. D. In *Homogeneous Catalysis, The Applications and Chemistry of Catalysis by Soluble Transition Metal Complexes*, Wiley: New York, 1992; p 56. (c) Al-Jarallah, A. H.; Anabtawi, J. A.; Siddiqui, M. A. B.; Aitani, A. M.; Al-Sadoun, A. W. *Catal. Today* **1992**, *14*, 1. (d) Bhaduri, S.; Mukesh, D. In *Homogeneous Catalysis, Mechanisms and Industrial Applications*; Wiley: New York, 2000; pp 142−147. (e) Vogt, D. Oligomerization of Ethylene to Higher Linear α-Olefins. In *Applied Homogeneous Catalysis with Organometallic Complexes*; Cornils, B., Herrmann, W. A., Eds.; VCH: Weinheim, Germany, 2002; pp 240−253.
(2) Hennico, A.; Leonard, J.; Forestire, A.; Glaize, Y. *Hydrocarbon Process.* **1990**, *69*, 73.
(3) (a) Tait, P. J. T.; Berry, I. G. In *Comprehensive Polymer Science*; Eastmond, G. C., Ledwith, A., Russo, S., Sigwalt, P., Eds.; Pergamon: Oxford, U.K., 1989; Vol. 4, p 575. (b) *Encyclopedia of Polymer Science and Engineering*; Mark, H. F., Bikales, N. B., Overberger, C. G., Menges, G., Kroschwitz, J. I., Eds.; Wiley: New York, 1986; Vol. 6, p 429.
(4) (a) Onsager, O.-T.; Johansen, J. E. In *The Chemistry of the Metal−Carbon Bond*; Hartley, F. R., Patai, F. R., Eds.; John Wiley & Sons: Chicester, U.K., 1986; Vol. 3, p 205. (b) Skupinska, J. *Chem. Rev.* **1991**, *91*, 613. (c) Olivier-Bourbigou, H.; Saussine, L. Dimerization and Codimerization. In *Applied Homogeneous Catalysis with Organometallic Complexes*; Cornils, B., Herrmann, W. A., Eds.; VCH: Weinheim, Germany, 2002; pp 253−265.

desirable, as it provides the wanted α-olefin in highest amount, while circumventing the separation. This has triggered intensive research in both academia and industry in recent years on the development of catalyst systems for the selective ethylene oligomerization. However, there has been only a limited number of catalyst systems thus far that oligomerize ethylene selectively to a certain linear α-olefin. These catalysts are based on chromium,[8−10] tantalum,[11] and titanium[12,13] and yield 1-hexene as the most common product.

The mono(cyclopentadienyl-arene)titanium [(η^5-C_5H_3R-(bridge)-Ar)$Ti^{IV}Cl_3$]/MAO (Ar = Ph, 4-MeC_6H_4, 3,5-$Me_2C_6H_3$; R = H, CMe_3, $SiMe_3$) systems with a hemilabile ancillary arene ligand have been reported recently as generators for a class of highly active catalysts for the selective trimerization of ethylene to 1-hexene.[13] The cationic [(η^5-C_5H_4-(CMe_2-bridge)-C_6H_5)Ti^{IV}-$(alkyl)_2$]$^+$ species with a dimethyl-substituted C_1 bridge and a pendant phenyl group has been shown as one of the most active precatalysts that almost entirely afford 1-hexene.[13b] We have recently reported a comprehensive theoretical mechanistic study for this precatalyst, exploring all crucial elementary steps of a tentative catalytic cycle that involves metallacycle intermediates (vide infra).[14] The original suggested mechanism by Hessen and co-workers[13a,b] (which is based on the first proposed metallacycle mechanism by Briggs and Jolly for the chromium-catalyzed process)[8,9] could be verified in important details but supplemented and extended by novel insights into how the linear oligomerization proceeds. First, a detailed insight into the discriminating factors for the observed high selectivity for ethylene trimerization has been provided; second, the role played by the hemilabile phenyl group has been elucidated; and third, the favorable path for precatalyst activation has been predicted, including the identification of the active catalyst species.[14] The ethylene oligomerization mediated by the same class of Ti catalysts has been also the subject of computational investigations by other groups, from which a basic understanding of the ethylene trimerization process has been revealed.[15]

It is the objective of the present study to probe computationally the catalytic capabilities of the heavier group 4 congeners for ethylene oligomerization with the cationic [(η^5-C_5H_4-(CMe_2-bridge)-C_6H_5)-$M^{IV}(alkyl)_2$]$^+$ species as precatalyst. To this end, a comprehensive investigation will be undertaken to explore the influence of group 4 metals on crucial elementary steps of both the oligomerization reaction course and of the initial process of precatalyst activation. The following questions are of interest in this regard. (1) How is the energy profile for the growth of metallacycle intermediates and for their decomposition into α-olefins affected by the variation of the metal? (2) Are the rates for these two processes quite similar or do they exhibit a nonuniform behavior as a function of the metallacycle size? (3) What is the largest possible size of metallacycle intermediates occurring in the reaction course? (4) Which step is rate-determining? (5) Which factors control the α-olefin distribution of the oligomerization process?

Addressing these questions will extend further the insights into the catalytic structure−reactivity relationships for the linear ethylene oligomerization supported by the title class of catalysts. It may furthermore lead us to suggest promising catalyst modifications aimed at (1) enhancing the catalytic ability for ethylene trimerization or (2) proposing a possible route for generation of 1-octene or a higher linear α-olefin as the predominant product. The influence of modification of the hemilabile arene functionality on the catalytic activity and selectivity will be the subject of a forthcoming investigation.

Computational Model and Method

Model. A tentative catalytic cycle originally proposed by Hessen and co-workers[13a,b] has been explored for the Ti catalyst, including all crucial elementary steps in our recent theoretical mechanistic study.[14] This investigation led us to suggest the refined catalytic cycle shown in Scheme 1 for the selective linear oligomerization of ethylene to 1-hexene. Metallacycle intermediates of different size are the crucial species of the catalytic cycle. The [(η^5-C_5H_3R-(bridge)-Ar)$Ti^{IV}Cl_3$] starting material requires activation with MAO that probably leads first to the cationic [(η^5-C_5H_4-(CMe_2-bridge)-C_6H_5)$Ti^{IV}Me_2$]$^+$ precatalyst via MAO-triggered alkylation and methyl/chlorine anion abstraction. The subsequent initialization process, where the precatalyst calls for activation while being transformed into the bis(ethylene)−Ti^{II} species, is predicted to involve the following sequence of steps: viz. first, ethylene insertion into the Ti^{IV}−Me bond of the precatalyst, followed by the concerted reductive β-H transfer under liberation of methane, and subsequent propylene displacement by ethylene accompanied with uptake of a second ethylene moiety. The oligomerization cycle is entered with the formation of the bis(ethylene)−Ti^{II} complex as the active catalyst species. The first titana(IV)cyclopentane is generated by oxidative coupling of the two coordinated ethylenes. Repeated ethylene uptake and subsequent insertion into the metallacycle increases its size, first giving rise to the titana(IV)cycloheptane. The decomposition of the metallacycle intermediates affording α-olefins proceeds via two distinct mechanisms. A stepwise mechanism comprising β-H abstraction and consecutive reductive CH elimination is operative for the conformationally rigid titana(IV)cyclopentane, while the conformationally

(5) For past reviews, see: (a) Keim, W.; Behr, A.; Röper, M. Alkene and Alkyne Oligomerization, Cooligomerization and Telomerization Reactions. In *Comprehensive Organometallic Chemistry*; Wilkinson, G., Stone, F. G. A., Abel, E. W., Eds.; Pergamon: New York, 1982; Vol. 8, pp 371−462. (b) Jolly, P. W. Nickel-Catalyzed Oligomerization of Alkenes and Related Reactions. In *Comprehensive Organometallic Chemistry*; Wilkinson, G., Stone, F. G. A., Abel, E. W., Eds.; Pergamon: New York, 1982; Vol. 8, pp 615−647.

(6) For recent reviews, see: (a) Britovsek, G. J. P.; Gibson, V. C.; Wass, D. F. *Angew. Chem., Int. Ed.* **1999**, *38*, 428. (b) Ittel, S. D.; Johnson, L. K.; Brookhart, M. *Chem. Rev.* **2000**, *100*, 1169. (c) Mecking, S. *Coord. Chem. Rev.* **2000**, *203*, 325. (d) Mecking, S. *Angew. Chem., Int. Ed.* **2001**, *40*, 534. (e) Gibson, V. C.; Spitzmesser, S. K. *Chem. Rev.* **2003**, *103*, 283.

(7) (a) Flory, P. J. *J. Am. Chem. Soc.* **1940**, *62*, 1561. (b) Schulz, G. V. *Z. Phys. Chem., Abt. B* **1935**, *30*, 379. (c) Schulz, G. V. *Z. Phys. Chem., Abt. B* **1939**, *43*, 25.

(8) Briggs, J. R. *J. Chem. Soc., Chem. Commun.* **1989**, 674.

(9) (a) Emrich, R.; Heinemann, O.; Jolly, P. W.; Krüger, C.; Verhovnik, G. P. J. *Organometallics* **1997**, *16*, 1511. (b) Jolly, P. W. *Acc. Chem. Res.* **1996**, *29*, 544.

(10) (a) Hogan, J. P. *J. Polym. Sci., Part A: Polym. Chem.* **1970**, *8*, 2637. (b) Manyik, R. M.; Walker, W. E.; Wilson, T. P. *J. Catal.* **1977**, *47*, 197. (c) Yang, Y.; Kim, H.; Lee, J.; Paik, H.; Jang, H. G. *Appl. Catal., A* **2000**, *193*, 29. (d) Köhn, R. D.; Haufe, M.; Kociok-Köhn, G.; Grimm, S.; Wasserscheid, P.; Keim, W. *Angew. Chem., Int. Ed.* **2000**, *39*, 4337. (e) Carter, A.; Cohen, S. A.; Cooley, N. A.; Murphy, A.; Scutt, J.; Wass, D. F. *Chem. Commun.* **2002**, 858. (f) McGuinness, D. S.; Wasserscheid, P.; Keim, W.; Morgan, D.; Dixon, J. T.; Bollmann, A.; Maumela, H.; Hess, F.; Englert, U. *J. Am. Chem. Soc.* **2003**, *125*, 5272. (g) McGuinness, D. S.; Wasserscheid, P.; Keim, W.; Hu, Ch.; Englert, U.; Dixon, J. T.; Grove, C. *Chem. Commun.* **2003**, 334. (h) Agapie, T.; Schofer, S. J.; Labinger, J. A.; Bercaw, J. E. *J. Am. Chem. Soc.* **2004**, *126*, 1304.

(11) Andes, C.; Harkins, S. B.; Murtuza, K. O.; Sen. A. *J. Am. Chem. Soc.* **2001**, *123*, 7423.

(12) Pellecchia, C.; Pappalardo, D.; Oliva, L.; Mazzeo, M.; Gruter, G.-J. *Macromolecules* **2000**, *33*, 2807.

(13) (a) Deckers, P. J. W.; Hessen, B.; Teuben, J. H. *Angew. Chem., Int. Ed.* **2001**, *40*, 2516. (b) Deckers, P. J. W.; Hessen, B.; Teuben, J. H. *Organometallics* **2002**, *21*, 5122. (c) The actual reaction conditions for the Ti-catalyzed selective trimerization of ethylene to 1-hexene are: 30 °C, ethylene pressure 5 bar, toluene as solvent. (d) The products of the Ti-catalyzed olefin trimerization are formed in 97% selectivity, comprising 83% of 1-hexene and 14% of 1-hexene/ethylene cooligomers.

(14) Tobisch, S.; Ziegler, T. *Organometallics* **2003**, *22*, 5392.

(15) (a) Blok, A. N. J.; Budzelaar, P. H. M.; Gal, A. W. *Organometallics* **2003**, *22*, 2564. (b) de Bruin, T. J. M.; Magna, L.; Raybaud, P.; Toulhoat, H. *Organometallics* **2003**, *22*, 3404.

Scheme 1. Theoretically Refined Catalytic Cycle for Selective Linear Oligomerization of Ethylene to 1-Hexene with a Cationic Cyclopentadienyl-Arene Titanium Precatalyst[14] (Based on a proposal by Hessen et al.)[13a,b]

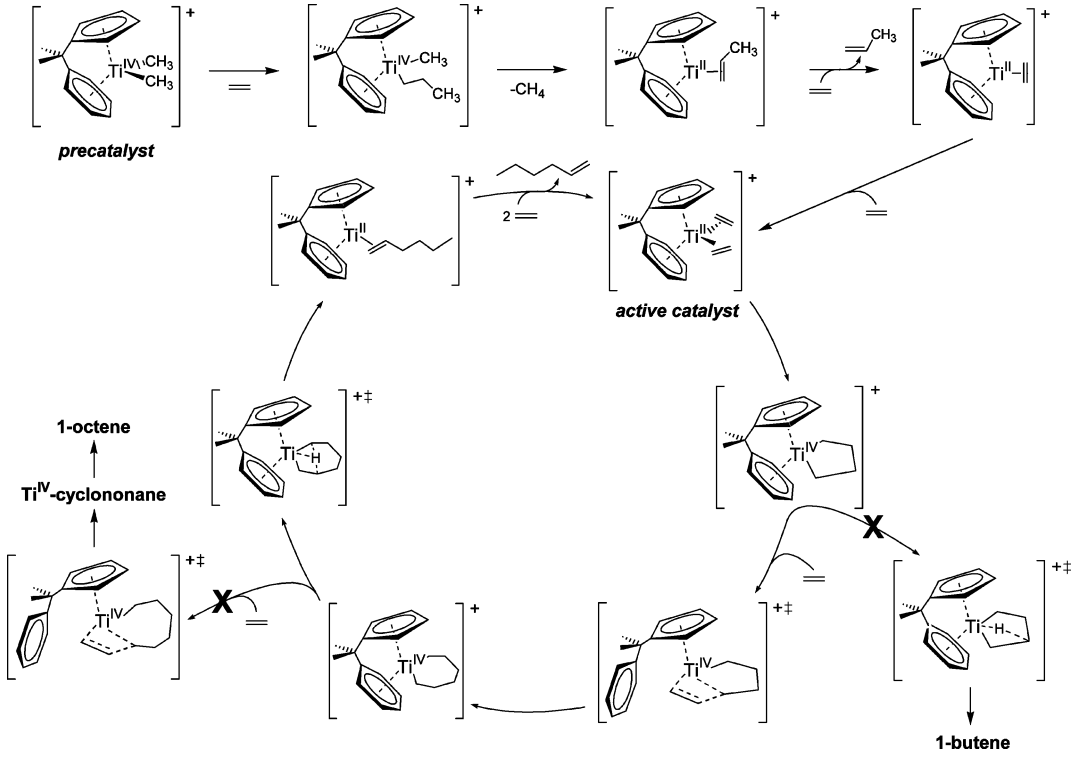

flexible larger titana(IV)cycles, starting with the seven-membered cycle, decompose by the concerted transition-metal-assisted β-H transfer. For the titana(IV)cyclopentane, further growth is predicted to be kinetically more favorable than the alternative decomposition affording 1-butene. The next larger titana(IV)cycloheptane intermediate, however, exhibits a reverse proclivity for the two processes. For this conformationally flexible metallacycle, its decomposition becomes significantly accelerated via the concerted route, which now is more facile than further titana(IV)cycle growth. As a consequence, (1) the seven-membered cycle is the largest titana(IV)cycle occurring in appreciable concentrations along the reaction course, and (2) 1-hexene is almost exclusively formed among the several possible ethylene oligomers. The catalytic cycle is closed via the facile 1-hexene displacement by new ethylene monomers, which regenerates the active catalyst complex. The hemilabile ancillary arene ligand has been demonstrated to play a critical role for making the metallacycle mechanism operable. The phenyl group acts (1) to counterbalance for the reduction and the increase of the coordination sphere around the titanium atom that accompanies the metallacycle growth and decomposition steps and (2) to stabilize the low formal Ti^{II} oxidation state through a notable back-bonding interaction.

All critical elementary processes of the oligomerization reaction cycle (cf. Scheme 1) have been explored theoretically for the cationic $[(\eta^5\text{-}C_5H_4\text{-}(CMe_2\text{-bridge})\text{-}C_6H_5)M^{II}(C_2H_4)_2]^+$ (M = Ti, Zr, Hf) active catalyst.[16] Metallacycle intermediates up to the 15-membered cycle were considered in the present investigation. Moreover, the favorable path for activation of the $[(\eta^5\text{-}C_5H_4\text{-}(CMe_2\text{-bridge})\text{-}C_6H_5)M^{IV}Me_2]^+$ precatalyst has been examined.

The effect of the solvent and the counterion was neglected in the present study. For the actual catalyst investigated here, the hemilabile ancillary arene functionality has been indicated to act so as to saturate the coordination sphere around the group 4 metal.[14] Accordingly, the catalyst−counterion interaction and specific influence of the solvent (toluene)[13c] can be assumed to be of minor relevance. This is confirmed by an overall negligible influence of both solvent and cocatalyst on the catalytic properties observed experimentally for the titanium-catalyzed process.[13b]

Method. All reported DFT calculations were performed by using the TURBOMOLE program package developed by Häser and Ahlrichs.[17] The local exchange-correlation potential by Slater[18a,b] and Vosko et al.[18c] was augmented with gradient-corrected functionals for electron exchange according to Becke[18d] and correlation according to Perdew[18e] in a self-consistent fashion. This gradient-corrected density functional is usually termed BP86 in the literature. In recent benchmark computational studies, it was shown that the BP86 functional gives results in excellent agreement with the best wave function-based methods available today, for the class of reactions investigated here.[19] The suitability of the BP86 functional for the reliable determination of the kinetic balance between the metallacycle growth and decomposition steps of the group 4 metal-assisted ethylene oligomerization has been demonstrated (cf. Supporting Information). In view of the fact that all species investigated in this study show a large HOMO−LUMO gap, a spin-restricted formalism was used for all calculations.

For group 4 elements we used the small-core Stuttgart−Dresden quasirelativistic effective core potentials with the associate [8s7p6d]/(6s5p3d) valence basis sets contracted according to a (311111/22111/411) scheme.[20] All other elements were represented by Ahlrichs' valence triple-ζ TZVP basis set[21b] with polarization functions on all atoms; viz.

(16) The energetics reported for the Ti catalyst deviate in some amounts from the previously reported values (ref 14), which is due to the different computational methodology employed (viz. different basis sets of equal quality than previously used and an improved treatment of entropic contributions for bimolecular association and dissociation steps occurring in condensed phase).

(17) (a) Ahlrichs, R.; Bär, M.; Häser, M.; Horn, H.; Kölmel, C. *Chem. Phys. Lett.* **1989**, *162*, 165. (b) Treutler, O.; Ahlrichs, R. *J. Chem. Phys.* **1995**, *102*, 346. (c) Eichkorn, K.; Treutler, O.; Öhm, H.; Häser, M.; Ahlrichs, R. *Chem. Phys. Lett.* **1995**, *242*, 652.
(18) (a) Dirac, P. A. M. *Proc. Cambridge Philos. Soc.* **1930**, *26*, 376. (b) Slater, J. C. *Phys. Rev.* **1951**, *81*, 385. (c) Vosko, S. H.; Wilk, L.; Nussiar, M. *Can. J. Phys.* **1980**, *58*, 1200. (d) Becke, A. D. *Phys. Rev.* **1988**, *A38*, 3098. (e) Perdew, J. P. *Phys. Rev.* **1986**, *B33*, 8822.; *Phys. Rev. B* **1986**, *34*, 7406.
(19) Jensen, V. R.; Børve, K. *J. Comput. Chem.* **1998**, *19*, 947.
(20) (a) Dolg, M.; Wedig, U.; Stoll, H.; Preuss, H. *J. Chem. Phys.* **1987**, *86*, 866. (b) Andrae, D.; Häussermann, M.; Dolg, M.; Stoll, H.; Preuss, H. *Theor. Chim. Acta* **1990**, *77*, 123.

for carbon a 11s/6p/1d set contracted to (62111/411/1) and for hydrogen a 5s/1p set contracted to (311/1). The frequency calculations were conducted by using Ahlrichs' split-valence SV(P) basis set[21a] with polarization functions on heavy atoms, but not on hydrogen; viz. for carbon a 7s/4p/1d set contracted to (511/31/1) and for hydrogen a 4s set contracted to (31), for SV(P)-optimized structures, which differ to a marginal extent from the TZVP-optimized ones. The corresponding auxiliary basis sets were used for fitting the charge density.[21c−e]

Stationary Points. The geometry optimization and the saddle-point search were carried out at the BP86 level of approximation by utilizing analytical/numerical gradients/Hessians according to standard algorithms. No symmetry constraints were imposed in any case. The stationary points were identified exactly by the curvature of the potential-energy surface at these points corresponding to the eigenvalues of the Hessian. All reported transition states possess exactly one negative Hessian eigenvalue, while all other stationary points exhibit exclusively positive eigenvalues. The educt and product that correspond directly to the located transition-state structure were verified by following the reaction pathway going downhill to both sides from slightly relaxed transition-state structures. The many isomers that are possible for each of the investigated species were carefully explored, with particular attention being given to the different conformers of the metallacycle intermediates. Only the most stable isomers of each of the key species were reported, for which the reaction and activation free energies (ΔG, $\Delta G^{\ddagger}$ at 298 K and 1 atm) were evaluated according to standard textbook procedures[22] using computed harmonic frequencies.

The oligomerization reaction occurs in liquid phase.[13c] Accordingly, the $T\Delta S$ contribution of ∼12 kcal mol^{-1} (298.15 K, 1 atm) calculated for ethylene coordination in gas phase certainly does not reflect the real entropic cost for association and dissociation of olefins under actual catalytic reaction conditions.[13c] The difference in the reaction entropy for the $L_nM + C_2H_4 \rightarrow C_2H_4{-}L_nM$ ethylene uptake process to occur in gas phase and condensed phase is mainly due to the ethylene solvation, since the solvation entropies of the L_nM educt and the $C_2H_4{-}L_nM$ ethylene adduct should be similar. The ethylene solvation entropy amounts to ∼16 eu in typical aromatic hydrocarbon solvents.[23] This reduces the entropic costs for ethylene complexation by ∼4.8 kcal mol^{-1} (298.15 K); thus, to about two-thirds of the gas-phase value. Therefore, the solvation entropy for olefin association and dissociation was approximated as being two-thirds of its gas-phase value, which is considered as a reliable estimate of the entropy contribution in condensed phase. This estimation agrees reasonably well with the findings of a recent theoretical study, where it was shown that for polar solvents the entropies in solution are decreasing to nearly half of the gas-phase value.[24]

Labeling of the Molecules. Uppercase Latin characters were used for species that participate along possible paths for transformation of the $Me_2{-}M^{IV}$ precatalyst **1** into the $(ethylene)_2{-}M^{II}$ active catalyst complex **2**, while crucial species of the catalytic ethylene oligomerization cycle were labeled with the following specific notation: viz. the metalla(IV)cycloalkanes **XC**; the respective ethylene π-adducts **XC-E**; the α-olefin-M^{II} complex **XC−O**. The notation **X** = **5**, **7**, **9**, **11**, **13**, **15** was used to indicate whether 5- 7-, 9-, 11-, 13-, or 15-membered metallacycle intermediates, i.e., metalla(IV)cyclo-pentane, -heptane, -nonane, -undecane, -tridecane, and -pentadecane, respectively, were involved.

We restricted the presentation of localized key species for the individual elementary steps to those for the Zr catalyst as a representative example. The key species for both Zr and Hf systems exhibit a very similar characteristic for crucial structural degrees of freedom. The respective key species for the Ti catalyst can be found in our previous study.[14]

Results and Discussion

We shall focus our discussion on the heavier group 4 congeners Zr and Hf and we will only refer to Ti systems for the purpose of comparison.[16] We start our investigation by evaluating the influence of group 4 metals on the precatalyst activation process. This is followed by the exploration of the formation and the growth of metallacycle intermediates and their decomposition. Here, our aim is twofold: first, to elucidate the influence of group 4 metals and second, to clarify how the size of the metallacycle affects the rates for both processes. In the final sections, an overall mechanistic picture for the three catalysts will be presented, which leads us to derive the factors that control the α-olefin product distribution. Furthermore, temperature is probed with respect to its ability to modulate the product distribution.

I. Precatalyst Activation. In this section, we study the initial transformation of the $Me_2{-}M^{IV}$ precatalyst **1** into the catalytically active bis(ethylene)−M^{II} complex **2**. The exploration of various conceivable pathways for the group 4 precatalysts revealed the same path (cf. Scheme 2) to be favorable as for the Ti system.[14] Commencing from **1**, ethylene insertion into the $M^{IV}{-}CH_3$ bond (**1** + $C_2H_4 \rightarrow$ **B**) is favorable compared to reductive CC elimination under ethane liberation (**1** → **A** + C_2H_6), as the latter step is kinetically distinctly more difficult ($\Delta\Delta G^{\ddagger}$ > 12.0 kcal mol^{-1}, cf. Scheme 2). This gives rise to the Me/Pr−M^{IV} species **B** in an exergonic, irreversible process. Species **B** is most likely to be converted into the propylene−M^{II} complex **C** by the concerted reductive β-CH elimination under liberation of methane (**B** → **C** + CH_4). Although imaginable, a stepwise pathway encountering a $H{-}M^{IV}$ species is not operable, as this species is found to be energetically highly unfavorable. It is therefore excluded from being part of the most feasible elimination pathway. The kinetically facile, moderately exergonic substitution of propylene by ethylene, together with the consecutive uptake of an additional ethylene monomer, leads to the active catalyst complex **2**. The alternative processes that commence from **B**, viz. ethylene insertion into the $M^{IV}{-}Pr$ bond (**B** + $C_2H_4 \rightarrow$ **E**), reductive CC elimination under butane liberation (**B** → **A** + C_4H_{10}), and reductive α-CH elimination with expulsion of methane (**B** → **F** + CH_4), are indicated to be kinetically disfavored. These steps are clearly not part of the most favorable path for precatalyst activation and possible ethylene coupling, and metathesis reactions initiated by the carbene−M^{II} species **F** are therefore entirely precluded because of an expected negligible thermodynamic population of **F**.

The first **1** + $C_2H_4 \rightarrow$ **B** ethylene insertion is seen to become kinetically more difficult for the Zr and Hf precatalysts relative to the Ti system ($\Delta G^{\ddagger}$ = 16.0 (Ti), 18.3 (Zr), and 19.0 (Hf) kcal mol^{-1}, cf. Scheme 2), and it is thermodynamically less favorable for the two heavier congeners as well. This is understandable from the fact that the M−C bond becomes stronger for the heavier group 4 metals.[25] The barrier for the **B**

(21) (a) Schäfer, A.; Huber, C.; Ahlrichs, R. *J. Chem. Phys.* **1992**, *97*, 2571. (b) Schäfer, A.; Huber, C.; Ahlrichs, R. *J. Chem. Phys.* **1994**, *100*, 5829. (c) Eichkorn, K.; Treutler, O.; Öhm, H.; Häser, M.; Ahlrichs, R. *Chem. Phys. Lett.* **1995**, *240*, 283. (d) Eichkorn, K.; Weigend, F.; Treutler, O.; Ahlrichs, R. *Theor. Chim. Acta* **1997**, *97*, 119. (e) TURBOMOLE basis set library.
(22) McQuarrie, D. A. *Statistical Thermodynamics*, Harper & Row: New York, 1973.
(23) Wilhelm, E.; Battino, R. *Chem. Rev.* **1973**, *73*, 1.
(24) Cooper, J.; Ziegler, T. *Inorg. Chem.* **2002**, *41*, 6614.
(25) (a) Mingos, D. M. P. *Essential Trends in Inorganic Chemistry*; Oxford University Press: Oxford, U.K., 1998. (b) Elschenbroich, Ch.; Salzer, A. *Organometallics*: *A Concise Introduction*, 2nd ed.; Wiley-VCH: Germany, 1992.

Scheme 2. Condensed Gibbs Free-Energy Profile (kilocalories per mole) of Competing Reaction Routes for Precatalyst Activation[a,b]

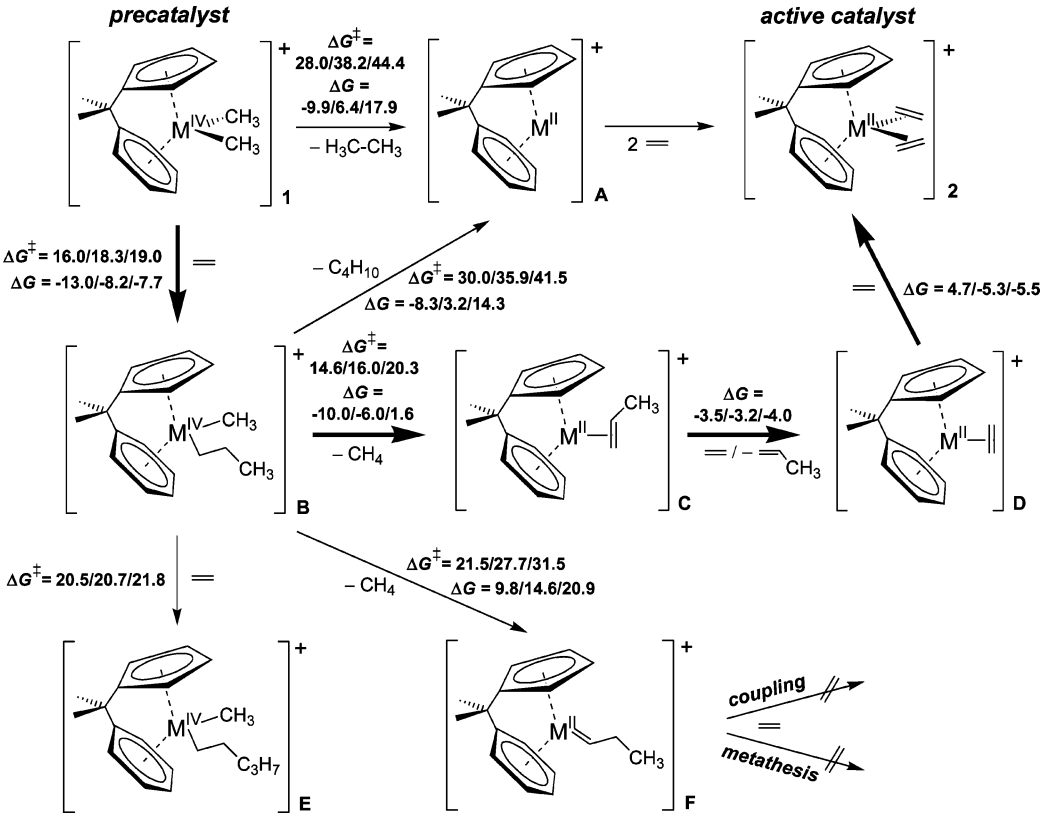

[a] The activation and reaction free energies for individual steps are given relative to the respective precursor for the Ti/Zr/Hf systems. [b] The favorable route is indicated by bold reaction arrows.

→ **C** + CH_4 reductive β-CH elimination increases in the same direction, but for the Hf precatalyst in a more pronounced fashion than found for the insertion step ($\Delta G^{\ddagger}$ = 14.6 (Ti), 16.0 (Zr), and 20.3 (Hf) kcal mol^{-1}, cf. Scheme 2). Furthermore, the thermodynamic driving force decreases in the order Ti > Zr > Hf. The β-CH elimination is moderately exergonic for the Ti system, while it is almost thermoneutral and reversible for Hf. The reductive elimination, a process that goes along with a formal reduction of the metal's oxidation state by two, becomes less facile upon going down group 4 (cf. Scheme 2). This can be rationalized in terms of an increased strength of the M−C bond on descending group 4. The same trends appear for the energy profile for the **B** → **F** + CH_4 α-CH elimination and, most noticeably, for the **1** → **A** + C_2H_6 CC elimination.

Ethylene insertion into the M^{IV}−propyl bond (**B** + C_2H_4 → **E**) requires a higher kinetic barrier than insertion into the M^{IV}−methyl bond (**1** + C_2H_4 → **B**). A kinetically slightly more difficult process can be expected for subsequent insertion events. This leads us to approximate the average free-energy barrier for ethylene insertion into the M^{IV}−alkyl bond to about ∼21.5 (Ti), ∼22.0 (Zr), and ∼23.0 (Hf) kcal mol^{-1}, respectively. The related growth of metallacycle intermediates by ethylene insertion into the M−C^{α} bond, however, is seen to be a more facile process with a distinctly smaller barrier ($\Delta\Delta G^{\ddagger}$ > 5.0 kcal mol^{-1} for Ti, Zr, and Hf, respectively, vide infra). This further corroborates that the metallacycle mechanism is operative for the group 4 catalysts investigated here,[26] while the alternative migratory insertion mechanism by Cossee and Arlman[27] must be considered to not be energetically feasible.

Different elementary processes are predicted to be connected with the overall highest activation free energy along the favorable path for precatalyst activation. For the Ti (16.0 kcal mol^{-1}) and Zr (18.3 kcal mol^{-1}) systems this is the **1** + C_2H_4 → **B** insertion, while the **B** → **C** + CH_4 reductive CH elimination is kinetically most expensive (20.3 kcal mol^{-1}) for the Hf congener. All these barriers are of the same magnitude or lower than the discriminating barrier of the oligomerization cycle (vide infra). Furthermore, the entire activation process is exergonic, driven by a thermodynamic force of −25.2 (Ti), −25.9 (Zr), and −19.6 (Hf) kcal mol^{-1}, respectively (ΔG for **1** + 3C_2H_4 → **2** + CH_4 + C_3H_6). This leads us to conclude that the **1** → **2** transformation is a smooth process, giving rise to appreciable concentrations of the active catalyst complex **2**, which should not discriminate the overall activity of the oligomerization process. A possible direction to facilitate the initial activation, especially for heavier group 4 congeners, is to substitute the $(alkyl)_2$−M^{IV} compounds by the well-known $(benzyl)_2$−M^{IV} complexes as precatalysts.[28] The ethylene insertion and reductive elimination steps can be expected to become kinetically less difficult in this case, since the M^{IV}−benzyl bond is likely to display a higher proclivity for both processes when compared to the M^{IV}−alkyl bond.

(26) (a) This may not be considered as a strict proof since we have not explicitly investigated termination of the M^{IV}−alkyl chain through β-H elimination affording α-olefins, which is likely to occur in a monomer-assisted process (ref 26b). (b) Margl, P.; Deng, L.; Ziegler, T. *J. Am. Chem. Soc.* **1999**, *121*, 154.

(27) (a) Cossee, P. *J. Catal.* **1964**, *3*, 80. (b) Arlman, E. J.; Cossee, P. *J. Catal.* **1964**, *3*, 99.

(28) (a) Sassmannshausen, J.; Powell, A. K.; Anson, C. E.; Wocadlo, S.; Bochmann, M. *J. Organomet. Chem.* **1999**, *592*, 84. (b) Deckers, P. J. W.; Hessen, B. *Organometallics* **2002**, *21*, 5564.

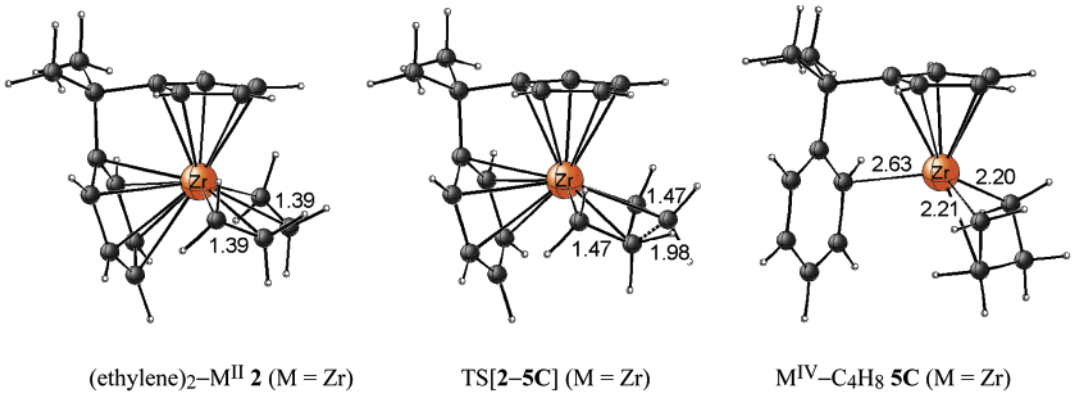

Figure 1. Selected geometric parameters (in angstroms) of the optimized structures of key species for oxidative coupling of two ethylene moieties in **2** to afford the metalla(IV)cyclopentane intermediate **5C**.[29] The parameters were exemplified for the Zr catalyst. The cutoff for drawing M−C bonds was arbitrarily set at 2.8 Å.

Table 1. Calculated Gibbs Free-Energy Profile (ΔG, $\Delta G^{\ddagger}$ in kilocalories per mole) for Formation and Growth of Group 4 Metallacycle Intermediates during the Linear Oligomerization of Ethylene Mediated by the Cationic [(η^5-C_5H_4-(CMe_2-bridge)-C_6H_5)$M^{II}(C_2H_4)_2]^+$ (M = Ti, Zr, Hf) Active Catalyst Complex[29,a]

cycle formation/growth	M	ΔG_{XC-E}[b]	$\Delta G^{\ddagger}$	ΔG
(ethylene)$_2$−M^{II} → M^{IV}−C_4H_8	Ti		5.3	−7.5
2 → **5C**	Zr		11.1	−5.5
	Hf		9.4	−5.1
M^{IV}−C_4 → M^{IV}−C_6H_{12}	Ti	10.3	15.6	−10.2
5C + C_2H_4 → **5C**−**E** → **7C**	Zr	5.0	11.5	−12.2
	Hf	4.8	11.8	−12.1
M^{IV}−C_6 → M^{IV}−C_8H_{16}	Ti	11.3	16.9	−4.0
7C + C_2H_4 → **7C**−**E** → **9C**	Zr	7.1	14.5	−5.3
	Hf	7.0	15.7	−5.2
M^{IV}−C_8 → M^{IV}−$C_{10}H_{20}$	Ti	14.4	16.5	−10.7
9C + C_2H_4 → **9C**−**E** → **11C**	Zr	12.6	17.3	−11.0
	Hf	12.4	17.4	−10.4
M^{IV}−C_{10} → M^{IV}−$C_{12}H_{24}$	Ti	13.9	16.1	−9.0
11C + C_2H_4 → **11C**−**E** → **13C**	Zr	12.5	17.2	−8.8
	Hf	12.1	16.4	−9.0
M^{IV}−C_{12} → M^{IV}−$C_{14}H_{28}$	Ti	12.7	14.8	−10.1
13C + C_2H_4 → **13C**−**E** → **15C**	Zr	11.8	16.1	−10.0
	Hf	11.6	15.1	−10.2

[a] The activation and reaction free energies for individual processes are given relative to {corresponding metalla(IV)cycle precursor + C_2H_4}. [b] Stabilization of the ethylene π-adduct **XC-E** (with X = 5, 7, 9, 11, 13, respectively).

II. Exploration of Crucial Elementary Processes. A. Formation of the Metalla(IV)cyclopentane through Oxidative Coupling. Formation of the first metalla(IV)cyclopentane **5C** occurs via oxidative coupling of the two ethylene moieties of the active catalyst complex **2**. The key species for this step are shown in Figure 1, and the energetics are part of Table 1. Commencing from **2**, the two coplanar ethylene moieties undergo oxidative addition under C−C bond formation through TS[**2**−**5C**] that emerges at a distance of ∼2.0 Å for the new C−C bond. The ancillary phenyl group, which is slightly asymmetrically coordinated to the metal in **2**, does not undergo a significant change of its coordination mode in the first stage of the process until the transition state is reached. The subsequent decay of TS[**2**−**5C**] into **5C**, however, goes along with reduction of the hapticity of the M−phenyl coordination, which is η^1 in **5C**, thereby indicating a weaker M−phenyl interaction in the formal M^{IV}−cycloalkane **5C** when compared to the (ethylene)$_2$−M^{II} **2** (cf. Figure 1).

The barrier for oxidative coupling is found to be decisively determined by the stability of **2**. The increasing stability upon going down group 4 suggests the highest barrier for the most stable (ethylene)$_2$−Hf^{II} catalyst species. Indeed, oxidative coupling is predicted to be kinetically more difficult for Zr and Hf, with $\Delta G^{\ddagger}$ = 11.1 and 9.4 kcal mol^{-1}, respectively, than for Ti ($\Delta G^{\ddagger}$ = 5.3 kcal mol^{-1}, cf. Table 1). The higher stability of the M−C olefin bond for the heavier group 4 homologues is likely to contribute to a larger barrier for these elements.

Overall, the first oxidative coupling is seen to be a highly facile and irreversible process, which is driven by a similar thermodynamic force of −(5−8) kcal mol^{-1} for all three group 4 catalysts. This indicates that **2**, after its generation during the initial precatalyst activation period, gets readily transformed into **5C**. Furthermore, formation of the first metalla(IV)cyclopentane is kinetically more facile than the subsequent ring enlargement through ethylene insertion (vide infra).

B. Growth of Metallacycle Intermediates. After formation of the first metalla(IV)cyclopentane **5C**, the cycle can grow further through a repeated sequence of consecutive ethylene uptake and insertion events, giving rise to the various metallacycle intermediates. Figure 2 displays, as a representative example, the key species for ring size enlargement of the metalla(IV)cycloheptane by two carbon atoms (i.e., **7C** + C_2H_4 → **9C**); the corresponding energetics are collected in Table 1. As a general feature of the metallacycle growth process, the π-adduct first formed by complexation of an ethylene monomer goes along with the displacement of the hemilabile arene functionality from the immediate proximity of the metal to accommodate the incoming ethylene. This has been indicated in our recent study[14] to be a smooth process, having a lower barrier than the subsequent insertion. The ancillary phenyl group still resides outside of the direct coordination sphere of the metal during ethylene insertion into the M^{IV}−C bond of the metallacycle. The corresponding transition-state structure comprises a quasi-planar four-membered cis arrangement of the metallacycle's M^{IV}−C bond, the coplanar oriented ethylene monomer and the metal, with the newly formed C−C σ-bond occurring at a distance of ∼2.2−2.4 Å. The decay of the TS into the next larger metallacycle leads to a reduction of the coordination number around the metal, which is compensated for by a more closely attached phenyl group in the M^{IV}−cycloalkanes (cf. Figure 2).

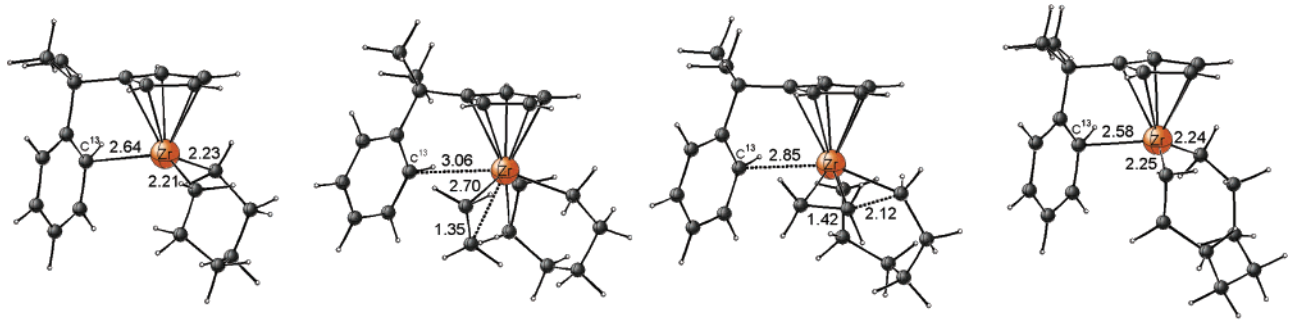

M^{IV}–C_6H_{12} **7C** (M = Zr) | $(C_2H_4)M^{IV}$–C_6H_{12} **7C-E** (M = Zr) | TS[**7C**–**9C**] (M = Zr) | M^{IV}–C_8H_{16} **9C** (M = Zr)

Figure 2. Selected geometric parameters (in angstroms) of the optimized structures of key species for ethylene insertion into the M^{IV}–C bond of the metalla(IV)cycloheptane **7C** giving rise to the metalla(IV)cyclononane intermediate **9C**.[29] The parameters were exemplified for the Zr catalyst. The cutoff for drawing M–C bonds was arbitrarily set at 2.8 Å.

The various group 4 metals are found to affect the reorganization of the metallacycle fragment and the coordination of the ancillary phenyl group in a different fashion. For titana(IV)cycles, the ligand rearrangement associated with ethylene π-adduct formation is of comparable extent for different ring sizes. This is apparent from the similar increase in the distance of the nearest M–phenyl contact by 0.7–1.0 Å, where this distance serves as an indicator for the strength of the M–phenyl interaction along the uptake step. The various Ti encounter complexes **XC-E** (with **X** = **5**, **7**, **9**, **11**, **13**) with a weakly interacting ethylene moiety are energetically unfavorable by ~3–6 kcal mol^{-1} at the enthalpic surface (ΔH for the **XC** + C_2H_4 → **XC-E** process, with **X** = **5**, **7**, **9**, **11**, **13**, M = Ti), which is found to be nearly independent of the ring size. The adducts **XC-E** must thus be transient species, not likely to occur in appreciable stationary concentrations. The unfavorable energetics of π-adduct formation are even more pronounced on the free-energy surface (~11–14 kcal mol^{-1}) because of the entropic cost for this bimolecular association step (cf. Table 1).

By contrast to this, a noticeably more modest ligand reorganization can be observed for ethylene complexation to the two smallest metalla(IV)cyclopentane and metalla(IV)-cycloheptane intermediates of Zr and Hf, as indicated by a phenyl ligand displacement of only ~0.2 and ~0.4 Å, respectively (cf. Figures 2, S1). For bigger zircona(IV)- and hafnia(IV)cycles starting with the nine-membered ring **9C**, however, a larger ligand reorganization, similar to that of the titana(IV)-cycles, is required. These findings can be traced back to the greater size of the heavier group 4 metals. Accordingly, ethylene coordinates most strongly to the smallest five-membered cycle **5C** (which is still unfavorable by ~5.0 kcal mol^{-1} at the free-energy surface) and, although in a lesser extent, to the next larger metalla(IV)cycloheptane **7C**. For larger zircona(IV)- and hafnia(IV)cycles, ethylene complexation is less favorable and similar to that of titana(IV)cycles (see Table 1).

The kinetics of the overall growth process consisting of ethylene uptake and insertion is determined by the total insertion barrier (i.e., relative to the metallacycle precursor + free ethylene). The entropic cost for ethylene association, which is due to the loss of translational and rotational degrees of freedom, is seen to contribute significantly to the barrier. The very similar activation free energies for the ethylene insertion of ~15–17 kcal mol^{-1} (cf. Table 1) for the successive increase of titana(IV)cycles point to uniform rates for these processes. The growth of zircona(IV)- and hafnia(IV)cycles, however, exhibits rates that depend on the actual ring size. The origin of this dependence, again, is strongly linked to the larger ionic radius of the heavier group 4 elements. Ethylene insertion into **5C** and **7C** is kinetically easiest with similar barriers for Zr and Hf species. The barrier amounts to ~11.6 kcal mol^{-1} ($\Delta G^{\ddagger}$) for the **5C** + C_2H_4 → **7C** step, and increases to ~15.1 kcal mol^{-1} ($\Delta G^{\ddagger}$) for the next **7C** + C_2H_4 → **9C** step (cf. Table 1). These first two insertion steps are predicted to be kinetically more difficult for titana(IV)cycles, thereby indicating a more facile formation of five- and seven-membered zircona(IV)- and hafnia(IV)cycles, relative to Ti counterparts. Inspection of the insertion profile for larger cycles reveals the following two aspects. First, starting with **9C**, nearly identical free-energy barriers of ~16.8 kcal mol^{-1} are computed for the further successive growth of zircona(IV)- and hafnia(IV)cycles, which second, is of the same magnitude as predicted for titana(IV)cycles (cf. Table 1).

Overall, uniform rates, being comparable for Ti, Zr, and Hf systems, can be expected for the growth of medium-sized metallacycles starting with **9C**. For catalysts with the heavier analogues Zr and Hf as active centers, the generation of only seven- and nine-membered metallacycles are kinetically more facile to some extent than the related Ti species.

Variation of the group 4 metal is seen to have a minor influence on the thermodynamics of the growth process. The heat of reaction for an individual insertion step is predicted to fall into a narrow range for all the catalysts, varying by only ~1 kcal mol^{-1} (with **5C** as an exception). The various metallacycles are formed in an exergonic, irreversible process driven by a thermodynamic force of −(4–12) kcal mol^{-1} (ΔG). The smallest heat of reaction for the formation of **9C** can be rationalized from the fact that the nine-membered ring represents the least favorable medium-sized ring.[30] Therefore, the M^{IV}–cycloalkanes should all be present in sufficient thermodynamic populations within the catalytic reaction course, taking here the

(29) M^{IV}–C_4H_8, M^{IV}–C_6H_{12}, M^{IV}–C_8H_{16}, M^{IV}–$C_{10}H_{20}$, M^{IV}–$C_{12}H_{24}$, and M^{IV}–$C_{14}H_{28}$ denote the metalla(IV)cyclopentane **5C**, -heptane **7C**, -nonane **9C**, -undecane **11C**, -tridecane **13C**, and -pentadecane **15C** intermediates, respectively.

(30) See, for instance: Allinger, N. L.; Cava, M. P.; de Jongh, D. C.; Johnson, C. R.; Lebel, N. A.; Stevens, C. L. *Organic Chemistry*; Worth: New York, 1976; p 40.

Scheme 3. Stepwise (top) and Concerted (bottom) Mechanism for Decomposition of Group 4 Metalla(IV)cycles Affording α-Olefins[a]

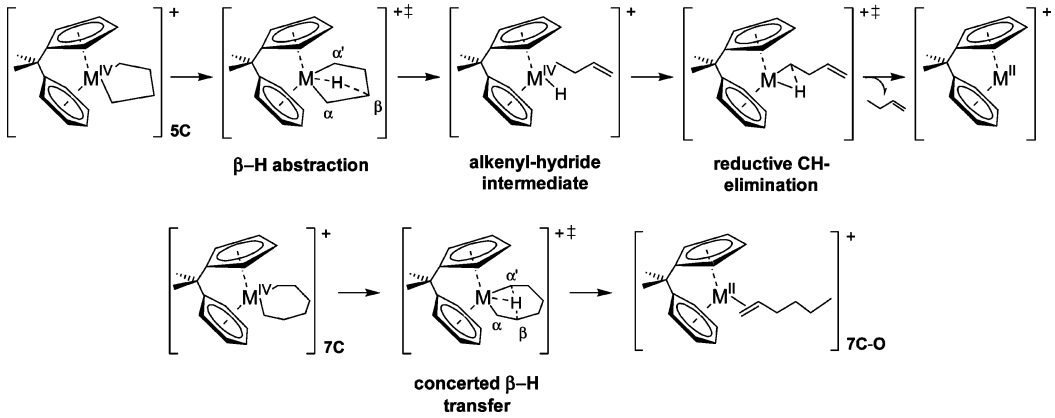

[a] The stepwise and concerted mechanisms are exemplified for five-membered, **5C**, and seven-membered, **7C**, cycles, respectively.

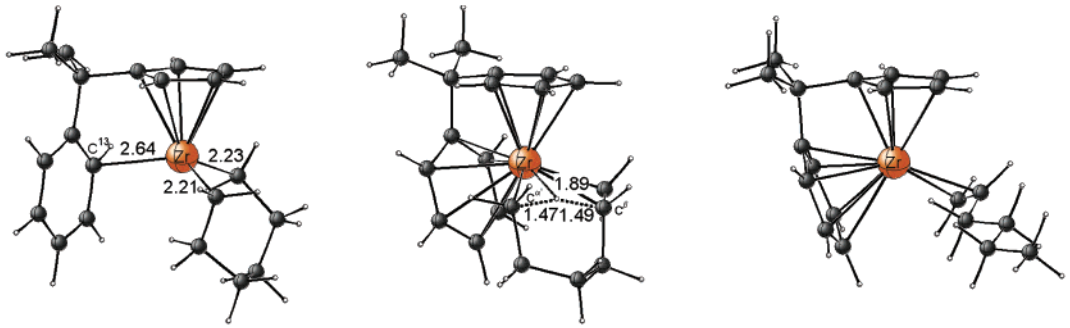

M^{IV}–C_6H_{12} **7C** (M = Zr) TS[**7C**–**7C-O**] (M = Zr) 1-hexene–M^{II} **7C-O** (M = Zr)

Figure 3. Selected geometric parameters (in angstroms) of the optimized structures of key species for decomposition of the metalla(IV)cycloheptane **7C** into the 1-hexene−M^{II} complex **7C-O** through concerted transition-metal-assisted β-H transfer.[29] The parameters were exemplified for the Zr catalyst. The cutoff for drawing M−C bonds was arbitrarily set at 2.8 Å.

competing decomposition process out of consideration. Accordingly, thermodynamics is clearly seen to not be the distinctive factor for the control of the α-olefin product distribution (cf. section III.A.).

C. Decomposition of Metallacycle Intermediates To Afford α-Olefins. The detailed investigation of several possible decomposition paths for zircona(IV)- and hafnia(IV)cycles reveals that the heavier congeners follow the same favorable paths that have been reported previously for titana(IV)cycles.[14] Depending on the actual size of the metallacycles, two distinct mechanisms are operative (Scheme 3). The stepwise mechanism consisting first of β-H abstraction and followed by reductive CH elimination with an intervening highly reactive alkenyl-hydride−M^{IV} species participating is favorable for the rigid **5C** species. This multistep process exhibits a double-valley energy profile, where the two subsequent abstraction and elimination steps have very similar kinetic barriers. By contrast, for the conformationally flexible metallacycles beginning with **7C** the concerted transition-metal-assisted β-H transfer ($C^{\beta} \rightarrow C^{\alpha'}$ hydrogen transfer) is operative and gives rise to a significant acceleration of the decomposition when compared to the process commencing from **5C**. As a consequence, the kinetically difficult decomposition of **5C** cannot compete with the **5C** + C_2H_4 → **7C** growth, such that the 1-butene generation path is of no relevance within the oligomerization course for any of the group 4 catalysts (as schematically indicated in Scheme 1 for the Ti catalyst).

Accordingly, we will focus the analysis of the decomposition of group 4 metallacycles entirely on medium-sized rings starting with **7C**. The key species involved along the concerted β-H transfer mechanism are exemplified in Figure 3 for the **7C** → **7C-O** step, and the energetics are summarized in Table 2. The favorable transition-state structure is described by a quasi-planar arrangement of the $MC^{\beta}HC^{\alpha'}$ fragment, where the hydrogen

Table 2. Calculated Gibbs Free-Energy Profile (ΔG, $\Delta G^{\ddagger}$ in kilocalories per mole) for Decomposition of Group 4 Metallacycle Intermediates Affording α-Olefins during the Linear Oligomerization of Ethylene Mediated by the Cationic $[(\eta^5\text{-}C_5H_4\text{-}(CMe_2\text{-bridge})\text{-}C_6H_5)M^{II}(C_2H_4)_2]^+$ (M = Ti, Zr, Hf) Active Catalyst Complex[29,a]

cycle decomposition	M	$\Delta G^{\ddagger}$	ΔG
M^{IV}−C_4H_8 → 1-butene-M^{II}	Ti	23.4	2.5
5C → **5C**−**O**	Zr	21.4	12.1
	Hf	25.7	21.8
M^{IV}−C_6H_{12} → 1-hexene-M^{II}	Ti	10.8	−11.0
7C → **7C**−**O**	Zr	13.1	−9.0
	Hf	17.4	−3.7
M^{IV}−C_8H_{16} → 1-octene-M^{II}	Ti	10.8	−18.7
9C → **9C**−**O**	Zr	16.1	−15.3
	Hf	20.1	−10.1
M^{IV}−$C_{10}H_{20}$ → 1-decene-M^{II}	Ti	17.4	−19.1
11C → **11C**−**O**	Zr	21.1	−15.4
	Hf	24.4	−11.1
M^{IV}−$C_{12}H_{24}$ → 1-dodecene-M^{II}	Ti	16.3	−21.5
13C → **13C**−**O**	Zr	21.1	−17.9
	Hf	24.5	−13.2

[a] The activation and reaction free energies for individual processes are given relative to the corresponding metalla(IV)cycle precursor.

atom, which is shifted in close proximity to the metal center, is at roughly equal distances from C^{β} and $C^{\alpha'}$. After crossing the TS, the concerted β-H transfer is completed with formation of the olefin−M^{II} complex **XC-O** (**X** = **7**, **9**, **11**, **13**). The ancillary phenyl ligand assists this process in two ways: by compensating for the decrease of coordination around the metal and by stabilizing the low M^{II} oxidation state (cf. Figure 3).

The individual group 4 metal influences the energy profile for decomposition in a pronounced way. Taking the decomposition of **7C** as an example, the modest free-energy barrier of 10.8 kcal mol^{-1} for the Ti catalyst increases by 2.3 and 6.6 kcal mol^{-1} for the Zr and Hf systems, respectively. At the same time, the process becomes thermodynamically less favorable in the order Ti > Zr > Hf, as indicated by the decreasing exergonicity of −11.0 (Ti), −9.0 (Zr), and −3.7 (Hf) kcal mol^{-1} (cf. Table 2). In contrast to the ethylene insertion step discussed in section II.B., electronic rather than geometrical factors are seen to be crucial for the rationalization of these findings. As already discussed for the reductive elimination steps involved in the initial precatalyst activation (cf. section I), again the enhanced M−C bond strength upon descending group 4 acts to disfavor the decomposition for heavier group 4 metals both kinetically and thermodynamically. A second factor that affects the kinetics, is some unfavorable close H−H contacts within the metallacycle fragment of the transition state for the larger rings. For titana(IV)cycles they become effective beginning with the 11-membered ring, giving rise to a significantly higher barrier ($\Delta\Delta G^{\ddagger}$ = 6.6 kcal mol^{-1} for **11C** → **11C-O** relative to **9C** → **9C-O**). Considering Zr and Hf systems, the H−H contacts are present, but are less pronounced in TS[**9C**−**9C-O**], while the TS for decomposition of larger cycles displays the same characteristic as the corresponding titana(IV)cycles do.

The analysis presented thus far leads us to the following conclusions. First, the metallacycle decomposition along the concerted pathway becomes kinetically as well as thermodynamically disfavored upon descending group 4. The **7C** → **7C-O** decomposition is predicted to be driven by the smallest thermodynamic force among all the concerted decomposition steps. This is understandable from the fact that the seven-membered cycle, which bears great similarity to the cyclohexane (cf. Figure 3), exhibits, like its organic counterpart,[30] the highest stability of all investigated metalla(IV)cycloalkanes. Second, the barriers exhibit a nonuniform behavior as a function of the ring size, and decomposition is predicted to become kinetically more difficult for larger metallacycles. Accordingly, for the investigated type of group 4 oligomerization catalysts, the catalytic ability of metallacycles to undergo degradation into the corresponding olefin−M^{II} complex becomes reduced for heavier group 4 metals and also for larger ring sizes.

III. The Entire Catalytic Reaction Course. A. Interrelation between Metallacycle Growth and Decomposition: Implications for the Selectivity of the Linear Ethylene Oligomerization. The following aspects are of crucial importance for the elucidation of the selectivity of the oligomerization process. On one hand, there is the concentration of the various possible metallacycles occurring within the reaction course, which is the thermodynamically related aspect. The propensity of an individual metallacycle intermediate either to increase its size by ethylene uptake and insertion or to decompose affording α-olefins, however, represents the kinetic aspect. As already analyzed in section II.B., the various metallacycles, which have been investigated up to the 15-membered ring, are likely to occur in appreciable thermodynamic populations, provided that repeated insertion events are feasible. Accordingly, thermodynamic factors cannot be effective for the regulation of the α-olefin product distribution. This led us to focus the following discussion entirely on kinetic aspects.

The insights into the crucial factors that determine the high selectivity of the Ti-based catalyst for ethylene trimerization, revealed from our recent study,[14] have already been summarized in the outline. The titana(IV)cycloheptane **7C** is the largest metallacycle occurring in appreciable concentrations during the oligomerization course. This is so because it exhibits a distinct higher propensity for β-H transfer affording 1-hexene compared to further ethylene insertion. As a further aspect, the **5C** + C_2H_4 → **7C** cycle growth step is connected with the overall highest barrier ($\Delta G^{\ddagger}$ = 15.6 kcal mol^{-1}, cf. Table 1),[16] which thereby must be considered as being rate-controlling.

The condensed free-energy profile of the Zr-mediated oligomerization, consisting of competing growth and decomposition steps starting with **5C**, is presented in Scheme 4. Decomposition of the first zircona(IV)cycle **5C**, which is readily formed via **2** → **5C** oxidative coupling (cf. section II.A.), along a stepwise pathway is seen to be kinetically disfavored when compared to the facile ethylene insertion ($\Delta\Delta G_{d-g}^{\ddagger}$ = 9.9 kcal mol^{-1}),[31] thereby preventing the occurrence of 1-butene as an oligomerization product. Comparable barriers are predicted for ethylene insertion and β-H transfer for the next two larger zircona(IV)cycles **7C** and **9C**, with the decomposition being slightly favorable kinetically ($\Delta\Delta G_{d-g}^{\ddagger}$ = −1.4 and −1.2 kcal mol^{-1}, respectively).[31] As a result, both 1-hexene and 1-octene will occur as products. The already mentioned steady increase of the β-H transfer barrier as a function of the ring size (cf. section II.C.), in combination with the nearly uniform kinetics for the growth process (cf. section II.B.), leads to a distinct retardation of the decomposition of larger zircona(IV)cycles ($\Delta\Delta G_{d-g}^{\ddagger}$ = 3.9 and 5.0 kcal mol^{-1} for **11C** and **13C**, respectively).[31] The significantly higher ability of 11- and 13-membered cycles for further growth, compared to decomposition, can reasonably be extrapolated to larger cycles as well. A simple kinetic model (cf. Supporting Information) that makes use of the computed barriers leads us to estimate the composition of the α-olefin products, which are summarized in Table 3. From this it can be seen that both 1-hexene and 1-octene are possible oligomer products, with 1-hexene likely to occur in about 90% abundance. Furthermore, 1-butene and α-olefins in the valuable range of C_{10}−C_{18} will not be formed. As a further aspect, the majority (∼99%, cf. Table 3) of the active species is consumed for the production of 1-hexene and 1-octene, such that the population of larger zircona(IV)cycles is very small. The Zr catalyst is interesting in that it is able to produce some 1-octene. However, this comes at the expense of a loss of the selectivity.

We should mention here that the computed energetic balance between the two processes includes some uncertainty, because of the estimate of entropic costs for monomer association and

(31) The $\Delta\Delta G_{d-g}^{\ddagger}$ value represents the difference of the free-energy barriers for decomposition and growth steps for a particular metallacycle (cf. Tables 1 and 2).

Scheme 4. Condensed Gibbs Free-Energy Profile (kilocalories per mole) of Competing Metalla(IV)cycle Growth and Decomposition Steps of the Linear Oligomerization of Ethylene by the Cationic $[(\eta^5\text{-}C_5H_4\text{-}(CMe_2\text{-bridge})\text{-}C_6H_5)M^{II}(C_2H_4)_2]^+$ (M = Zr) Active Catalyst[a,b,c]

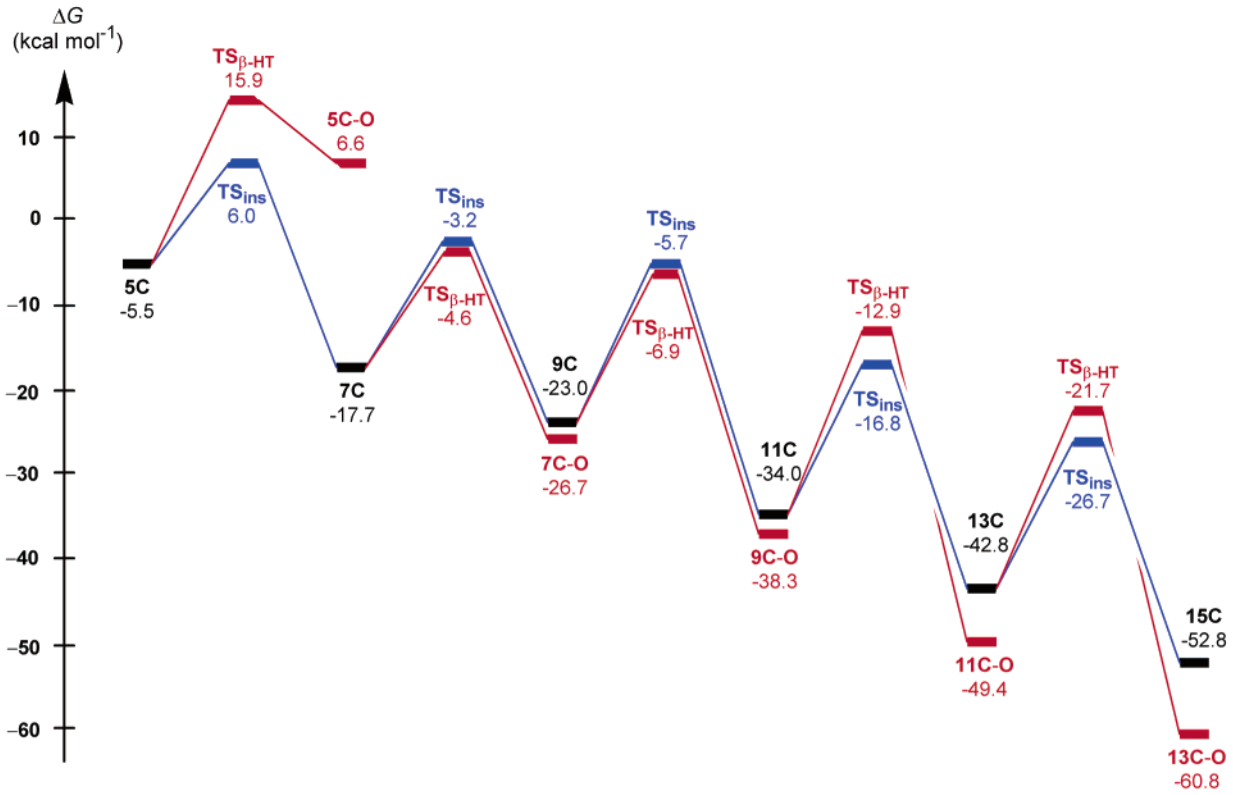

[a] The sequence of steps starts with the five-membered cycle **5C**. [b] Free energies are given relative to **2** corrected by the respective number of ethylene molecules. [c] Blue and red are used to mark metalla(IV)cycle growth and decomposition, respectively.

Table 3. Estimated Composition of the α-Olefin Products and Abundance of Metallacycle Intermediates for the Linear Oligomerization of Ethylene Mediated by the Cationic $[(\eta^5\text{-}C_5H_4\text{-}(CMe_2\text{-bridge})\text{-}C_6H_5)M^{II}(C_2H_4)_2]^+$ (M = Zr, Hf) Active Catalyst Complex[29]

α-olefin	1-butene	1-hexene	1-octene	1-decene	1-dodecene
$M^{IV}-C_nH_{2n}$	$M^{IV}-C_4H_8$	$M^{IV}-C_6H_{12}$	$M^{IV}-C_8H_{16}$	$M^{IV}-C_{10}H_{20}$	$M^{IV}-C_{12}H_{24}$
M = Zr					
%(α-olefin)[a]	5.5E-6	91.4	7.6	1.4E-3	2.1E-4
$[M^{IV}-C_nH_{2n}]$[b]	100	100	8.6	1.0	1.0
M = Hf					
%(α-olefin)[a]	6.4E-9	5.4	1.0	1.3E-4	1.2E-5
$[M^{IV}-C_nH_{2n}]$[b]	100	100	94.6	93.6	93.6

[a] Portions of individual α-olefins in the product mixture, estimated according to eq 1 (cf. Supporting Information). [b] Thermodynamic abundance of various metallacycles, estimated according to eq 2 (cf. Supporting Information), with the population of the metalla(IV)cyclopentane $M^{IV}-C_4H_8$ assumed to be 100.

dissociation processes occurring in condensed phase.[32] The prediction of accurate free energies for transition-metal-assisted processes in condensed phase remains still a challenge for computational chemistry. Therefore, the estimated α-olefin composition might be regarded as a rough approximation, though the promising ability of the Zr catalyst for 1-octene production is clearly apparent. On the other hand, we are not able to make a definite prediction as to which step has to be considered as being rate-controlling for the Zr-catalyzed oligomerization. However, we consider the difference in the barriers for β-H transfer and insertion of $>\sim$4 kcal mol^{-1} ($\Delta\Delta G_{d-g}^{\ddagger}$)[31] computed for **5C**, **11C**, and **13C** to be large enough to discriminate between the two competing processes.

From the condensed free-energy profile given in Scheme 5, it becomes evident that for the Hf-mediated oligomerization the ethylene insertion into an individual hafnia(IV)cycle is predicted to always be connected with a lower barrier than the β-H transfer. Furthermore, the energy gap ($\Delta\Delta G_{d-g}^{\ddagger}$)[31] increases with the enlargement of the ring size and amounts to 1.7 (**7C**), 2.7 (**9C**), 8.0 (**11C**), and 9.4 (**13C**) kcal mol^{-1}, respectively. Therefore, for all hafnia(IV)cycle intermediates further ring enlargement is likely to be the favorable process. The computed $\Delta\Delta G_{d-g}^{\ddagger}$ value clearly reveals that decomposition of **11C** and **13C** is almost entirely suppressed kinetically, while the seven- and nine-membered cycles (although to a lesser extent for **9C**) should exhibit some ability to decompose into 1-hexene and 1-octene, respectively. As revealed from the estimated oligomer distribution (cf. Table 3), similar to the findings for the Zr catalyst, the fraction of C_6-C_{18} chain lengths consists predominantly of 1-hexene together with some 1-octene (cf. Table 3),

(32) Furthermore, for the bimolecular growth step the rate does also depend on the ethylene concentration. For an assumed 1 M concentration (i.e., corresponding to an ethylene pressure of 24.5 atm), this can be considered as being of negligible influence, such that the barriers for growth and decomposition can reasonably be compared.

Scheme 5. Condensed Gibbs Free-Energy Profile (kilocalories per mole) of Competing Metalla(IV)cycle Growth and Decomposition Steps of the Linear Oligomerization of Ethylene by the Cationic $[(\eta^5\text{-}C_5H_4\text{-}(CMe_2\text{-bridge})\text{-}C_6H_5)M^{II}(C_2H_4)_2]^+$ (M = Hf) Active Catalyst[a]

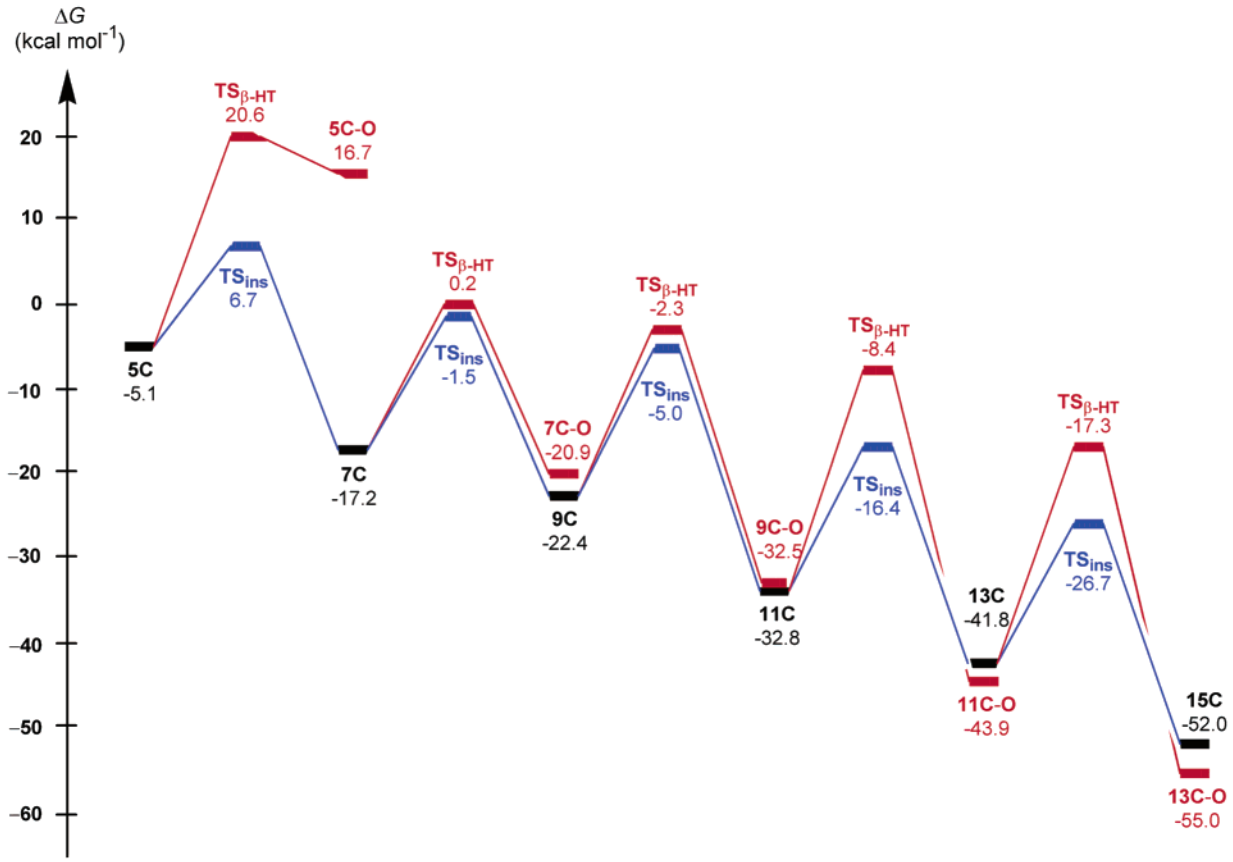

[a] See footnotes for Scheme 4.

which, however, is distinctly smaller than for the Zr-catalyzed process, while 1-butene and oligomers of chain lengths $C_{10}-C_{18}$ should not occur. In sharp contrast to the Zr system, however, for the Hf catalyst a substantial amount (>∼90%, cf. Table 3) of the active species is transformed into larger metallacycles, thereby being unproductive for generation of α-olefins in the valuable range of C_6-C_{18} chain lengths. This may afford long-chain oligomers and polymers ($\gg C_{20}$ chain lengths) as the prevalent product fraction. This points out that the Hf catalyst, when compared to the Zr analogues, should display a significantly lower productivity for generation of 1-hexene/1-octene. Furthermore, the general increase of the decomposition barrier in the order Zr < Hf (cf. section II.C.) indicates the Hf catalyst to be also less active. As a further important aspect of mechanistic concern, the hafnia(IV)cycle decomposition is predicted to be rate-determining, which is in contrast to the situation for the Ti catalyst.

The analysis of the two crucial insertion and decomposition steps for zircona(IV)- and hafnia(IV)cycles presented thus far leads us to the following conclusions. (1) Neither the Zr nor the Hf catalyst is found to assist oligomerization of ethylene to a specific α-olefin, as the Ti-based trimerization catalyst does. (2) For these catalysts, the oligomer distribution of C_6-C_{18} chain lengths is likely to consist predominantly of 1-hexene together with smaller amounts of 1-octene, while 1-butene and α-olefins of chain lengths $C_{10}-C_{18}$, if generated at all, should occur only in negligible portions. For the Hf-catalyzed process, long-chain oligomers and polymers can be expected as the prevalent product fraction. (3) Between the group 4 catalysts of the investigated type, the Zr system appears as the most promising candidate having catalytic potential for production of 1-octene, although not selectively.

B. Temperature Influence on the α-Olefin Product Distribution. After elucidating the critical factors that regulate the oligomer product distribution, the influence of the temperature is examined next. Temperature can reasonably be assumed to have a distinct influence on the product distribution since the bimolecular growth and the unimolecular decomposition processes are likely to be affected at elevated temperature in a different fashion. We shall concentrate here on the two competing processes with **7C** and **9C** as the corresponding precursor species, which have been analyzed in the previous section as the crucial steps that decisively control the oligomer product composition. Table 4 collects the corresponding free-energy barriers computed over a temperature range between 25 and 300 °C.

The *β*-H transfer is seen to become kinetically slightly more difficult at elevated temperatures. This is understandable from the fact that a higher ordered transition state participates in this process (cf. Figure 3), thereby giving rise to a negative entropy of activation. The ethylene insertion step, as could be expected, is affected by temperature in a more pronounced fashion, giving rise to a more rapid increase of the barrier for insertion than for *β*-H transfer at elevated temperatures. Thus, the barrier for growth will rise more rapidly with temperature than the barrier for decomposition.[32]

For the Zr-catalyzed oligomerization, **7C** and **9C** are predicted to exhibit a slightly higher ability for decomposition than for

Table 4. Calculated Temperature Dependence of the Activation Free Energies ($\Delta G^{\ddagger}$ in kilocalories per mole) for Growth and Decomposition of Group 4 Metallacycle Intermediates Involved in the Linear Oligomerization of Ethylene Mediated by the Cationic $[(\eta^5\text{-}C_5H_4\text{-}(CMe_2\text{-bridge})\text{-}C_6H_5)M^{II}(C_2H_4)_2]^+$ (M = Ti, Zr, Hf) Active Catalyst Complex[29,a]

cycle growth	M	$\Delta G^{\ddagger}$ 298/323/373/473/573 K
$M^{IV}-C_6 \rightarrow M^{IV}-C_8H_{16}$	Ti	16.9/17.7/19.2/22.5/25.2
7C + $C_2H_4 \rightarrow$ **7C**−**E** → **9C**	Zr	14.5/15.3/16.9/20.1/23.4
	Hf	15.7/16.5/18.2/21.4/24.6
$M^{IV}-C_8 \rightarrow M^{IV}-C_{10}H_{20}$	Ti	16.5/17.2/18.6/21.4/24.2
9C + $C_2H_4 \rightarrow$ **9C**−**E** → **11C**	Zr	17.3/18.0/19.4/22.3/25.1
	Hf	17.4/18.1/19.5/22.5/25.4
cycle decomposition	**M**	**$\Delta G^{\ddagger}$ 298/323/373/473/573 K**
$M^{IV}-C_6H_{12} \rightarrow$ 1-hexene-M^{II}	Ti	10.8/10.9/11.0/11.3/11.6
7C → **7C**−**O**	Zr	13.1/13.3/13.7/14.4/15.2
	Hf	17.4/17.6/18.0/18.8/19.6
$M^{IV}-C_8H_{16} \rightarrow$ 1-octene-M^{II}	Ti	10.8/10.8/10.9/11.0/11.2
9C → **9C**−**O**	Zr	16.1/16.2/16.4/16.9/17.3
	Hf	20.1/20.2/20.4/21.0/21.6

[a] The activation free energies for individual processes are given relative to the corresponding metalla(IV)cycle precursor (decomposition step) and to {respective metalla(IV)cycle precursor + C_2H_4} (growth step), respectively.

Table 5. Temperature Influence on the Estimated Composition of the α-Olefin Products and Abundance of Metallacycle Intermediates for the Linear Oligomerization of Ethylene Mediated by the Cationic $[(\eta^5\text{-}C_5H_4\text{-}(CMe_2\text{-bridge})\text{-}C_6H_5)M^{II}(C_2H_4)_2]^+$ (M = Zr, Hf) Active Catalyst Complex[29]

α-olefin	1-hexene 298/323/373/473/573 K	1-octene 298/323/373/473/573 K
$M^{IV}-C_nH_{2n}$	$M^{IV}-C_6H_{12}$	$M^{IV}-C_8H_{16}$
M = Zr		
%(α-olefin)[a]	91.4/96.0/98.7/99.8/99.9	7.6/3.8/1.3/0.2/7.4E-2
$[M^{IV}-C_nH_{2n}]$[b]	100/100/100/100/100	8.6/4.0/1.3/0.2/7.4E-2
M = Hf		
%(α-olefin)[a]	5.4/14.8/56.7/94.1/98.8	1.0/2.9/9.9/4.9/1.2
$[M^{IV}-C_nH_{2n}]$[b]	100/100/100/100/100	94.6/85.2/43.3/5.9/1.2

[a,b] See Table 3 footnotes.

further growth at standard conditions (i.e., negative $\Delta\Delta G_{d-g}^{\ddagger}$ value at 298 K, cf. Scheme 4). Therefore, the cycle growth becomes distinctly disfavored at higher temperatures, as pointed out by an increasing $\Delta\Delta G_{d-g}^{\ddagger}$ gap[31] of −2.0/−3.2/−5.7/−8.2 kcal mol^{-1} at 50/100/200/300 °C for **7C**, as an example (cf. Table 4). This is furthermore revealed from the estimated relative α-olefin composition (cf. Table 5), where the 1-hexene portion is seen to increase at higher temperatures. Overall, elevated temperatures are acting here to retard further growth of **7C**, which is likely to be almost entirely suppressed at temperatures above 150 °C (i.e., 1-hexene portion >99%, cf. Table 5), thereby switching the Zr system into a highly selective catalyst for ethylene trimerization.

In the case of the Ti catalyst, higher temperatures lead also to larger negative $\Delta\Delta G_{d-g}^{\ddagger}$ values (cf. Table 4). However, raising the temperature is not likely to increase the selectivity of the already highly selective trimerization catalyst further, since a $\Delta\Delta G_{d-g}^{\ddagger}$ gap for **7C** of −6.1 kcal mol^{-1} (25 °C, cf. Table 4) can be considered to be large enough to prevent occurrence of any larger titana(IV)cycle intermediate.

The situation is different for the Hf catalyst, where a crossover in the size of the barriers for the growth and decomposition steps is suggested to occur at ∼100 °C and ∼150 °C for **7C** and **9C**, respectively (cf. Table 4). Assuming a high thermal catalyst stability, the decomposition is indicated to become favorable at 200/300 °C by $\Delta\Delta G_{d-g}^{\ddagger}$ = 2.6/5.0 and 1.5/3.8 kcal mol^{-1} for **7C** and **9C**, respectively (cf. Table 4). Furthermore, temperature is seen to influence the $\Delta\Delta G_{d-g}^{\ddagger}$ gap in a similar fashion for **7C** and **9C**. Both aspects are reflected in the estimated relative 1-hexene/1-octene proportions (cf. Table 5). This lead us to conclude that (1) temperatures of ∼300 °C, thus distinctly higher than estimated for the Zr-based catalyst, are required to force the Hf catalyst to produce 1-hexene nearly selectively and that (2) lower temperatures in the range of 50−150 °C, however, are not likely to modulate the 1-hexene/1-octene distribution.

Overall, for the investigated Zr- and Hf-based oligomerization catalysts, elevated temperatures can act at best to switch their catalytic abilities to support ethylene trimerization almost selectively, but is not likely to modulate the oligomer product composition toward an enhanced 1-octene portion.

Concluding Remarks

We have presented a detailed computational analysis of the catalytic abilities of heavier group 4 (M = Zr, Hf) metals for linear ethylene oligomerization with the cationic $[(\eta^5\text{-}C_5H_4\text{-}(CMe_2\text{-bridge})\text{-}C_6H_5)M^{IV}(CH_3)_2]^+$ complex as precatalyst, employing a gradient-corrected DFT method. The parent Ti system has been reported as a highly selective catalyst for ethylene trimerization,[13] the origin of which has been elucidated in recent theoretical mechanistic studies.[14,15] To the best of our knowledge, this is the first comprehensive theoretical exploration of the ethylene oligomerization with the group 4 metals Ti, Zr, and Hf as the active centers, where all crucial elementary steps of the catalytic cycle have been critically scrutinized. This allowed us to deduce the catalytic potential of the Zr and Hf systems for production of higher linear α-olefins, which have not been reported thus far by experimental groups.

An identical sequence of steps was found for Zr and Hf to convert the Me_2-M^{IV} precatalyst **1** into the $(ethylene)_2-M^{II}$ active catalyst complex **2**; viz. ethylene insertion into the M^{IV}−Me bond, the concerted reductive β-H transfer under liberation of methane, and consecutive propylene displacement by ethylene together with uptake of a second ethylene monomer. The overall transformation occurs in a smooth fashion, giving rise to sufficient concentrations of **2**, which thereby is not likely to influence the activity of the oligomerization process.

The mechanism involving metallacycle intermediates, originally proposed by Briggs and Jolly,[8,9] has been supported by the present study to be operative for the investigated class of group 4 catalysts, while the "coordination−migratory" mechanism by Cossee and Arlman[27] is indicated to not be energetically feasible.

The energy profile for the subsequent growth of metallacycle intermediates through ethylene uptake and insertion into the $M^{IV}-C$ bond displays a distinct characteristic for the various group 4 catalysts. Nearly uniform rates can be assumed for the investigated five- to 13-membered titana(IV)cycles, since the insertion barriers fall into a narrow range of ∼15−17 kcal mol^{-1} ($\Delta G^{\ddagger}$). Concerning the Zr and Hf systems, the ethylene insertion is found to be particularly facile for the two smallest five-, **5C**, and seven-membered, **7C**, cycles, which is clearly attributed to the larger ionic radius of heavier group 4 metals. The generation of larger metallacycles starting with **9C**, however, should occur

at uniform rates that moreover are indicated as being comparable for all three group 4 catalysts.

The thermodynamic driving force for an individual insertion event is the same to within ~1 kcal mol^{-1} for the different group 4 metals. All metallacycles are formed in an exergonic, irreversible process. Accordingly, they are likely to occur in appreciable thermodynamic populations, provided that repeated insertions are being feasible. Furthermore, thermodynamic factors are less likely to be effective for the regulation of the oligomer product distribution, which is found to be entirely controlled kinetically, viz. by the propensity of an individual metallacycle to grow further or to decompose, affording the respective α-olefin.

The metallacycle decomposition through the concerted β-H transfer becomes kinetically as well as thermodynamically disfavored upon descending group 4. In contrast to the insertion step, electronic factors, not geometrical, are seen to be crucial. The increase of the M−C bond strength in the order Ti < Zr < Hf causes the decomposition to be more difficult for the heavier group 4 homologues. Also, unfavorable H−H contacts occurring in the metallacycle fragment of the TS for larger cycles do retard the β-H transfer further.

Our theoretical investigation reveals a catalytic ability of the Zr and Hf systems that is different from the parent highly selective Ti catalyst for ethylene trimerization. Neither Zr nor Hf is found to assist ethylene oligomerization to a specific α-olefin. The oligomer distribution of the Zr-mediated reaction is likely to comprise predominantly 1-hexene together with some 1-octene, while 1-butene and α-olefins of chain lengths C_{10}−C_{18} should occur only in negligible portions. A similar composition of the small C_6−C_{18} α-olefin fraction is indicated for the Hf catalysts, but with long-chain oligomers and polymers as the prevalent products. Between the group 4 catalysts of the investigated type, the Zr system appears as the most promising candidate having catalytic potential for production of 1-octene, although not selectively.

Temperature is seen acting to modulate the oligomer distribution. Elevated temperatures of ~150 and ~300 °C will force both the Zr and Hf systems, respectively, into highly selective catalysts for ethylene trimerization. On the other hand, ambient temperatures are not likely to modulate the oligomer product composition toward an enhanced 1-octene portion.

The present investigation will be continued with a forthcoming investigation of the influence of modification of the hemilabile arene functionality on the catalytic activity and selectivity of group 4 ethylene oligomerization catalysts.

Acknowledgment. Support from the National Science and Engineering Research Council of Canada (NSERC) is gratefully acknowledged. T.Z. wishes to thank the Canadian government for a Canada research chair in theoretical inorganic chemistry.

Supporting Information Available: Full descriptions of the geometry of all reported species (Cartesian coordinates in angstroms). Also included is the pictorial representation of key species for ethylene insertion into the M^{IV}−C bond of the metalla(IV)cyclopentane intermediate (Figure S1). This material is available free of charge via the Internet at http://pubs.acs.org.

JA048861L